From flatness-based trajectory tracking to path following

Moritz Werling
University of Karlsruhe (TH)
Institute of Applied Computer Science/Automation
76128 Karlsruhe, Germany
moritz.werling@iai.fzk.de

Lutz Gröll
Forschungszentrum Karlsruhe (FZK)
Institute of Applied Computer Science
76021 Karlsruhe, Germany
lutz.groell@iai.fzk.de

***Abstract*— In this contribution, we develope a flatness-based control strategy suitable for parking assistance and autonomous maneuvering in static environments. It is derived from quasi-static trajectory tracking control in a straight-forward manner and preserves the invariance property (with respect to the choice of the initial frame) of the plant for the closed loop system. In addition, it solves the nearest-point projection of the car onto the curve implicitly. The results are illustrated by simulation and experiment.**

***Index Terms*— Flatness-based path tracking, quasi-static feedback, automated parking, autonomous vehicle**

I. Introduction

The problem of automated vehicle guidance needs to be solved for both modern driving assistance systems and fully autonomous vehicles. As a matter of fact, tracking control of the nonholonomic car is one of the most often studied examples in flatness-based control, e. g. [2]. In this context, the control objective is tracking a desired position $\vec{y}_d(t)$ over time (*trajectory tracking*, Fig. 1(a)) what hinders the transfer to practice since very accurate longitudinal input dosing (gas, break) is required. For automated parking and autonomous maneuvering in static environments however, the control objective can be modified to minimizing the distance to a given curve $\mathcal{C}_d$ (*path tracking, path following*, Fig. 1(b)) at any longitudinal movement. This minimization has to be solely realized by the application of the steering wheel, whereas the velocity is affected by either the responsible driver (parking assist) or a separate longitudinal controller (autonomous application).

As already depicted in Fig. 1(b), for feeding back the tracking error to a reference position in the control law, the nearest-point projection of the car onto the path has to be continuously solved by the minimization problem

$$s^{\perp}(t) = \underset{s_c}{\operatorname{argmin}} \parallel \mathcal{C}_d(s_c) - \vec{y}(t) \parallel_2, \qquad (1)$$

with $\vec{y}(t)$ the current car position and s_c the arc length parameter of $\mathcal{C}_d$.

In this contribution the path tracking as well as the projection problem will be solved:
Section II introduces the simplified nonholonomic vehicle dynamics and describes its invariance property. In contrast to [5], where *control of the clock* is applied, the invariance under $SE(2)$ (planar rotations and translations) of the plant is taken advantage of. From the flatness-based design of the tracking controllers in Sec. II two path tracking control laws along with an observer-like projection method are derived in Sec. IV and compared in Sec. V. The most promising algorithm is then implemented and tested on an experimental vehicle which is described in Sec. VI. Section VII concludes with a summary.

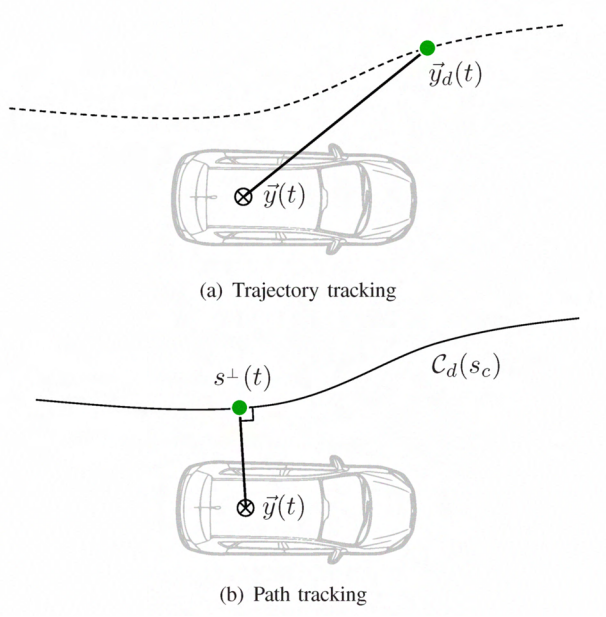

(a) Trajectory tracking

(b) Path tracking

Fig. 1. Different control objectives

II. Nonholonomimic vehicle dynamics and $SE(2)$-invariance

The mathematical model of the car dynamics at low speed results from virtually combining the front and rear wheels in each case to an intermediate one and assuming rolling without slipping. Then the car carries out a rotation around its instantaneous center C according to Fig. 2.

Complying with the notation in Fig. 2, the differential equations can be written in the form

$$\begin{bmatrix} \dot{\vec{y}} \\ \dot{\theta} \end{bmatrix} = v \begin{bmatrix} \vec{t} \\ u_\delta \end{bmatrix}$$

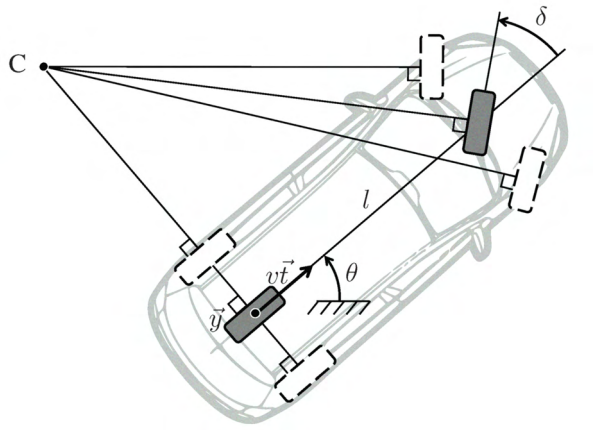

Fig. 2. Nonholonomic car model

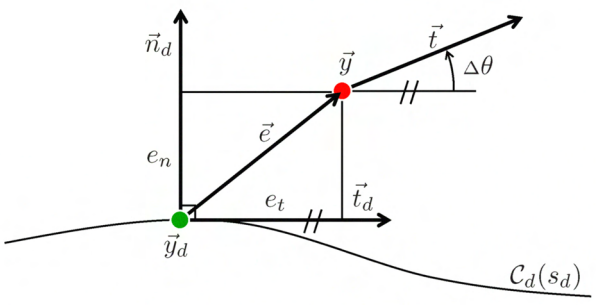

Fig. 3. Definition of the scalar invariant errors

with the input substitution

$$u_\delta = \frac{\tan\delta}{l} \tag{2}$$

and the tangent vector $\vec{t}$ given by

$$\vec{t} = \begin{bmatrix} \cos\theta \\ \sin\theta \end{bmatrix}, \qquad \dot{\vec{t}} = \dot{\theta}\vec{n}, \qquad \vec{n} = \begin{bmatrix} -\sin\theta \\ \cos\theta \end{bmatrix}.$$

Obviously, two trajectories resulting from the same control $[0,T] \ni t \mapsto (v(t),\delta(t))^T \in \mathbb{R}^2$ but from different initial positions and orientations of the car, can be transformed into each other according to the fundamental theorem of planar curves. This implies that the car is invariant under the action of the elements of the group $SE(2)$, and can be easily verified by calculation.

Because any kind of internal dynamics (zero dynamics as a special case, [3]) might lead to a collision (e. g. the car rear cutting corners), the differential flatness property [2] of the nonholonomic car is most useful and taken into account in the following.

III. Invariant Trajectory Tracking

According to [6], the invariance property of the car means in a nutshell that there is an invariant tracking output error of the car which can be stabilized by feedback (e. g. *quasi-static* feedback [1]).

The invariant tracking error $\vec{e}_{\text{inv}}$ be now defined as the parallel and perpendicular projection of the tracking error onto the curve in the desired position $\vec{y}_d$ [7], namely

$$\vec{e}_{\text{inv}} = \begin{bmatrix} e_t \\ e_n \end{bmatrix} = \begin{bmatrix} \langle \vec{e}, \vec{t}_d \rangle \\ \langle \vec{e}, \vec{n}_d \rangle \end{bmatrix}, \tag{3}$$

which can be seen in Fig. 3.

A. Time scaling

In order to avoid the well-known difficulties at $v = 0$, we design the controller with a new independent variable σ instead of the physical time t. The relation between the derivative w.r. t. t and the one w.r. t. σ is given by

$$\frac{\mathrm{d}}{\mathrm{d}t} = \frac{\mathrm{d}\sigma}{\mathrm{d}t} \cdot \frac{\mathrm{d}}{\mathrm{d}\sigma} = \dot{\sigma}\frac{\mathrm{d}}{\mathrm{d}\sigma}. \tag{4}$$

B. Time scaling with $\sigma = s_d$

With $\sigma = s_d$ (covered arc length of the desired position with $0 \overset{!}{<} \dot{s}_d$), (4) becomes $\frac{\mathrm{d}}{\mathrm{d}t} = \dot{s}_d \frac{\mathrm{d}}{\mathrm{d}s_d}$. With the new longitudinal input

$$\xi = v/\dot{s}_d, \tag{5}$$

the model dynamics can be rewritten as

$$\begin{bmatrix} \vec{y}\,' \\ \theta' \end{bmatrix} = \xi \begin{bmatrix} \vec{t} \\ u_\delta \end{bmatrix},$$

whereas $()'$ denotes in this section the derivation w.r. t. s_d. For the sake of clarity we introduce the angle $\Delta\theta := \sphericalangle(\vec{t}, \vec{t}_d)$ with

$$\Delta\theta := \theta - \theta_d, \quad \langle \vec{t}, \vec{t}_d \rangle = \cos\Delta\theta, \quad \langle \vec{t}, \vec{n}_d \rangle = \sin\Delta\theta.$$

Following quasi-static feedback design method, the feedback law can now be derived by differentiating the components of $\vec{e}_{\text{inv}}$ twice w.r. t. s_d and applying Frenet Formulas:

$$\begin{aligned} e_t' &= \frac{\mathrm{d}}{\mathrm{d}s_d}\langle \vec{e}, \vec{t}_d \rangle = \langle \vec{e}\,', \vec{t}_d \rangle + \langle \vec{e}, \vec{t}_d\,' \rangle \\ &= \langle \vec{y}\,' - \vec{y}_d\,', \vec{t}_d \rangle + \langle \vec{e}, \kappa_d \vec{n}_d \rangle \\ &= \langle \xi\vec{t}, \vec{t}_d \rangle - \langle \vec{t}_d, \vec{t}_d \rangle + \kappa_d \langle \vec{e}, \vec{n}_d \rangle \\ &= \xi\cos\Delta\theta - 1 + \kappa_d e_n \qquad (6) \\ e_n' &= \xi\sin\Delta\theta - \kappa_d e_t \qquad (7) \\ e_t'' &= \xi'\cos\Delta\theta - \xi\Delta\theta'\sin\Delta\theta + \kappa_d' e_n + \kappa_d e_n' \\ &= \xi'\cos\Delta\theta - \xi(u_\delta\xi - \kappa_d)\sin\Delta\theta + \kappa_d' e_n + \kappa_d e_n' \qquad (8) \\ e_n'' &= \xi'\sin\Delta\theta + \xi(u_\delta\xi - \kappa_d)\cos\Delta\theta - \kappa_d' e_t - \kappa_d e_t', \qquad (9) \end{aligned}$$

whence $\Delta\theta' = \theta' - \theta_d' = u_\delta\xi - \kappa_d$, with κ_d the curvature described by $\vec{y}_d(t)$. The linearizing input is chosen

$$e_t' =: w_t; \qquad e_n'' =: w_n.$$

Solving (6) for ξ gives the linearizing feedback in longitudinal direction

$$\xi = \frac{w_t + 1 - \kappa_d e_n}{\cos\Delta\theta}, \tag{10}$$

and combining (8), (9) to

$$\begin{aligned} e_n'' \cos\Delta\theta - e_t'' \sin\Delta\theta &= w_n \cos\Delta\theta - w_t' \sin\Delta\theta = \\ &\underbrace{(\cos\Delta\theta \sin\Delta\theta - \sin\Delta\theta \cos\Delta\theta)}_{=0} \xi' \\ &+ \underbrace{(\cos^2\Delta\theta + \sin^2\Delta\theta)}_{=1} \xi (u_\delta \xi - \kappa_d) \\ &- (\kappa_d' e_t + \kappa_d e_t') \cos\Delta\theta - (\kappa_d' e_n + \kappa_d e_n') \sin\Delta\theta \end{aligned}$$

yields

$$u_\delta = \frac{1}{\xi^2} \left\langle \begin{bmatrix} -\sin\Delta\theta \\ \cos\Delta\theta \end{bmatrix}, \begin{bmatrix} -e_n & -e_n' \\ e_t & e_t' \end{bmatrix} \begin{bmatrix} \kappa_d' \\ \kappa_d \end{bmatrix} + \begin{bmatrix} w_t' \\ w_n \end{bmatrix} \right\rangle + \frac{\kappa_d}{\xi}, \tag{11}$$

which completes the computation of the feedback.

Exponential stabilization of the tracking error can be achieved by

$$w_t = -k_t e_t; \quad w_n = -k_{n1} e_n' - k_{n0} e_n, \tag{12}$$

$0 < k_t, k_{n1}, k_{n0}$. The derivative w_t' in (11) can easily be calculated by differentiating the stabilization (12):

$$w_t' = -k_t e_t' = -k_t w_t \tag{13}$$

The real plant input (δ, v) can finally be calculated from (2) and (5).

Clearly, there exist two singularities corresponding to large tracking errors: one at $\Delta\theta = \pm\pi$ in (10), the other when $\xi = 0$ in (11), which is the same as

$$-k_t e_t + 1 - \kappa_d e_n = 0,$$

and therefore depends on the parameter k_t.

C. Time scaling with $\sigma = s$

This time we chose the covered distance of the rear wheel center

$$s(t) = \int_0^t |v(\tau)| \mathrm{d}\tau$$

to be the independent variable. Notice the absolute value, which asserts $0 < \dot{s}(t)$ during backward-driving. Let $\varsigma \in \{-1; 1\}$ according to the engaged gear. With

$$\begin{aligned} \vec{y}\,' &= \varsigma \vec{t}; \qquad \theta' = \varsigma u_\delta \\ \eta &:= \dot{s}_d / |v|, \end{aligned} \tag{14}$$

the error dynamics transform into

$$\begin{aligned} e_t' &= \frac{\mathrm{d}}{\mathrm{d}s} \langle \vec{e}, \vec{t}_d \rangle = \langle \vec{y}\,' - \vec{y}_d\,', \vec{t}_d \rangle + \langle \vec{e}, \vec{t}_d\,' \rangle \\ &= \langle \varsigma \vec{t}, \vec{t}_d \rangle - \langle \eta \vec{t}_d, \vec{t}_d \rangle + \langle \vec{e}, \eta \kappa_d \vec{n}_d \rangle \\ &= \varsigma \cos\Delta\theta - \eta(1 - \kappa_d e_n) && (15) \\ e_n' &= \varsigma \sin\Delta\theta - \eta \kappa_d e_t && (16) \\ e_t'' &= -\varsigma \Delta\theta' \sin\Delta\theta - \eta'(1 - \kappa_d e_n) \\ &\quad + \eta(\kappa_d' e_n + \kappa_d e_n') && (17) \\ e_n'' &= \varsigma \Delta\theta' \cos\Delta\theta - \eta' \kappa_d e_t - \eta(\kappa_d' e_t + \kappa_d e_t') && (18) \\ \Delta\theta' &= \varsigma u_\delta - \eta \kappa_d. && (19) \end{aligned}$$

Keep in mind that here $()' = \frac{\mathrm{d}}{\mathrm{d}s} = \frac{\mathrm{d}s_d}{\mathrm{d}s} \frac{\mathrm{d}}{\mathrm{d}s_d} = \frac{\dot{s}_d}{\dot{s}} \frac{\mathrm{d}}{\mathrm{d}s_d} = \eta \frac{\mathrm{d}}{\mathrm{d}s_d}$, so that $\kappa_d' = \eta \frac{\mathrm{d}}{\mathrm{d}s_d} \kappa_d$.

The new input $e_t' =: w_t$; $e_n'' =: w_n$ leads with (15) to

$$\eta = \frac{\varsigma \cos\Delta\theta - w_t}{1 - \kappa_d e_n}, \tag{20}$$

and with (17), (18), and (19) to

$$\begin{aligned} u_\delta = &\frac{(1 - \kappa_d e_n)(w_n + \eta(\kappa_d e_t)') - \kappa_d e_t (w_t' - \eta(\kappa_d e_n)')}{(1 - \kappa_d e_n)\cos\Delta\theta + \kappa_d e_t \sin\Delta\theta} \\ &+ \varsigma \eta \kappa_d. \end{aligned} \tag{21}$$

The stabilization and computation of the original plant input can be analogously carried out to the last section. However, the singularity in the denominator of (21) does not have parameter dependencies and can be rewritten to

$$\frac{e_n - \frac{1}{\kappa_d}}{e_t} = \tan\Delta\theta.$$

In combination with the singularity of (20) there is a clear physical interpretation: the car moves either straight towards, away from, or directly above the desired instantaneous center C_d, s. Fig. 4. Also notice the singularity at $\eta = 0$ when solving (14) for $|v|$. As we will not carry out this calculation in the path controller of Sec. IV, we do not pay attention to it here.

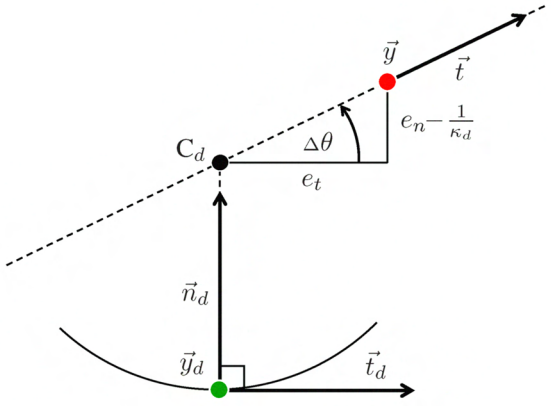

Fig. 4. Geometric interpretation of the singularities

IV. Transfer to Path Control

A. Switching cause and effect

Considering the feedback-controlled longitudinal movement the *reaction* to the movement of the desired position (*cause*), this chain has to be obviously turned around for the path tracking problem: We need the reference point on the curve (formerly desired position) to follow the car, so that the lateral error e_t is minimized. Mathematically speaking, this can be easily done by solving (5) and (14) respectively for $\dot{s}_d$ - without touching the error dynamics. In order to

avoid confusion, the subscript $()_d$ (*desired*) is changed to $()_c$ (*curve*). This yields

$$\dot{s}_c = \frac{1}{\xi} v \qquad \text{for } \sigma = s_c \tag{22}$$

$$\dot{s}_c = \eta |v| \qquad \text{for } \sigma = s. \tag{23}$$

The current velocity v is now a measured variable (s. Fig. 5). Notice, that $\xi \approx 1$ if the car is in a neighborhood of the reference point on the curve.

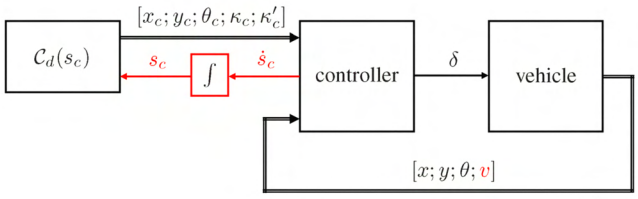

Fig. 5. Block diagram of path tracking controller

Figure 6 and 7 demonstrate the approach with the two different control laws in a numeric simulation: The vehicle starts in both cases with an initial lateral error $e_n = 1.0\,\text{m}$ to the curve and the reference point is initialized with a longitudinal error $e_t = 0.25\,\text{m}$. As the vehicle starts to move with a sinusoidal velocity profile, both the lateral and the longitudinal errors decay exponentially in their respective σ-domain (Fig. 7, bottom). Due to the chosen parameters, this happens ten times as fast in the longitudinal direction as in the lateral direction. After a couple of driven centimeters, the lateral error is practically zero and the reference point on the curve is the closest to the vehicle. Additionally, the vehicle controlled in the s_d-domain is depicted in time-equidistant stop-motion along with the corresponding reference point on $\mathcal{C}_d$.

B. Suppression of the lateral error dynamics

With $e_t(t) \equiv 0$ the dynamics corresponding to the s_d-domain controller become

$$\begin{aligned} w_t &= w_t' = 0; \qquad \xi^{\perp} = \frac{1 - \kappa_c e_n}{\cos \Delta\theta}; \\ e_n' &= \xi^{\perp} \sin \Delta\theta = (1 - \kappa_c e_n) \tan \Delta\theta, \end{aligned}$$

and (11) simplifies to

$$u_{\delta\xi}^{\perp} = \frac{(e_n \kappa_c' + e_n' \kappa_c) \sin \Delta\theta + w_n \cos \Delta\theta}{{\xi^{\perp}}^2} + \kappa_c \frac{\cos \Delta\theta}{1 - \kappa_c e_n}. \tag{24}$$

Analogous calculations for the s-domain controller (21) lead to

$$u_{\delta\eta}^{\perp} = \frac{w_n}{\cos \Delta\theta} + \kappa_c \frac{\cos \Delta\theta}{1 - \kappa_c e_n}. \tag{25}$$

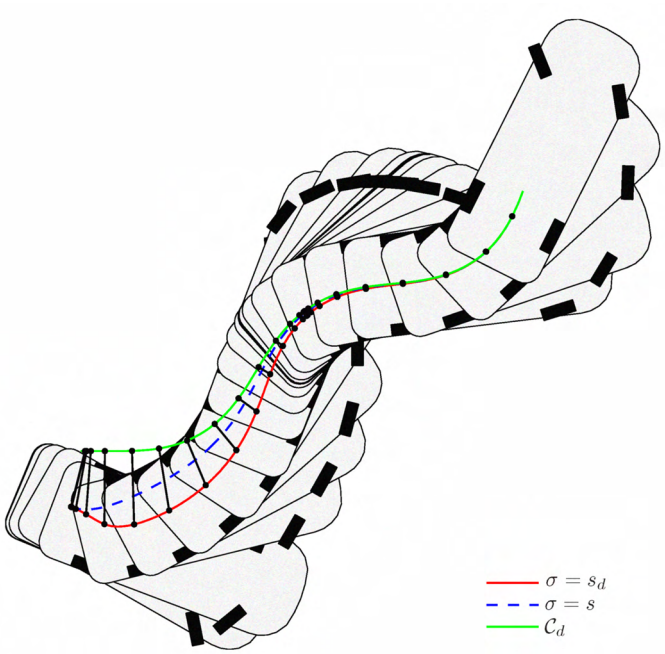

Fig. 6. Path tracking with an initial error

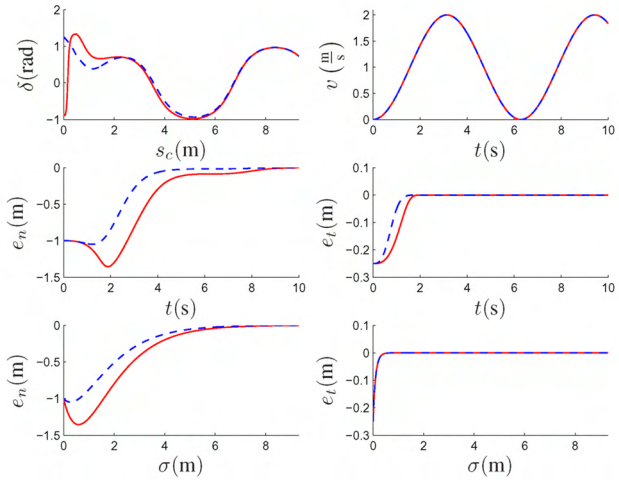

Fig. 7. Simulation plots associated with Fig. 6

V. Discussion

Starting off with trajectory tracking, both time-scaling methods prove successful with regard to eliminating the singularity at $v = 0$. The lateral and longitudinal error dynamics can be independently assigned by a proper choice of the control parameters, so no *gain alignment* [6] is required. Close to the desired position $\vec{y}_d$ the two controllers perform identical as can be seen from linearization[1]. However, as big lateral and longitudinal errors become significant, e. g. during experimentation, fault diagnostics,

[1]Due to the invariant error definition, linearization about $\mathcal{C}_d$ ($\sin\theta_d, \kappa_d e_t, \kappa_d e_n \approx 0$; $\xi, \eta, \cos\Delta\theta \approx 1$) seems worth considering. Yet, the effort for the determination of the convergence region exceeds the implementation savings by far.

or in the presence of strong disturbances, the singularity in the s_d-domain becomes an issue. On the contrary, the singularities in the s-domain are so far off from the desired behavior of the car (s. Fig. 4) that they can be practically excluded.

As for the path tracking problem, the projection onto the curve $\mathcal{C}_d$ is solved implicitly, meaning instead of the distance, the longitudinal error e_t was minimized by $\dot{s}_c$, which leads to the same result. This bears resemblance to an (nonlinear) observer for $s^{\perp}$. Here likewise, the path tracking controller in the s-domain proves advantageous: The time constant in lateral direction can be chosen fairly small, so that the lateral error vanishes quickly, whereas the parameter dependant singularity in the s_d-domain prohibits a high gain, as otherwise $\dot{s}_d < 0$ and the system would destabilize.

The lateral control laws for path tracking are identical to trajectory tracking. However, in case of a known $s_{c0} = s_c(t{=}0)$ or in combination with a closed/numeric solution of the minimization problem (1), $e_t \equiv 0$ can be assumed. The simplified control laws (24) and (25) perform identical to the original ones, even though the $\frac{\mathrm{d}\kappa}{\mathrm{d}s_c}$-term does not appear in the s-domain control law. This lowers the differentiable requirements for $\mathcal{C}_d$ by one degree and so facilitates path planning. The control law (24) was therefore chosen for implementation in the next section.

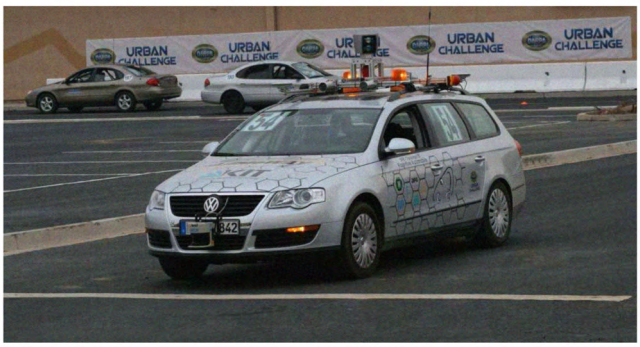

Fig. 8. Experimental vehicle *AnnieWAY*

VI. Experimental results

A Volkswagen Passat (s. Fig. 8), known as *AnnieWAY* [4] from the 2007 *Darpa Urban Challenge*, with by-wire steering, throttle, and breaking, serves as experimental vehicle. The controller is implemented on a dSpace real-time environment and the self-localization bases on a GPS/INS navigation system supported by odometry. Figure 9 shows the results of a backward parallel parking maneuver at walking speed. Despite curvatures of the planned path close to the turn radius of the car, the tracking error e_t was kept under 0.01 m (assuming "ground truth" of the self-localization). For the sake of clearness, the steering wheel angle δ_w is depicted.

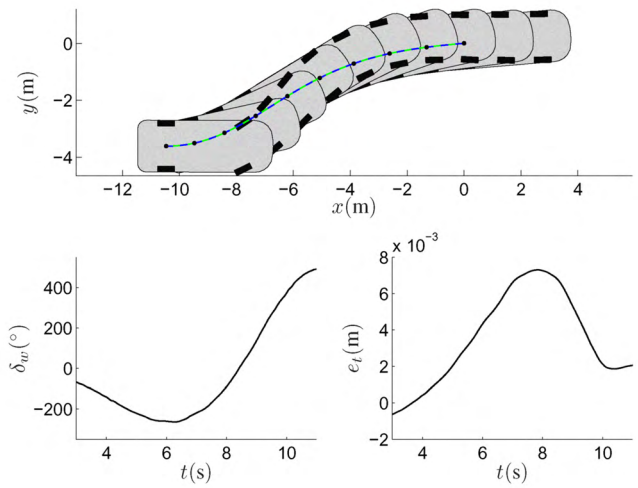

Fig. 9. Practical tracking performance in a backward parking maneuver

VII. Conclusions

In this paper an approach to flatness-based invariant path tracking was introduced. Based on the nonholonomic car model, two different trajectory tracking laws with different error dynamics were derived and converted to path tracking controllers, meeting the specifications of automated parking and autonomous maneuvering in a static environment. The projection problem onto the curve was implicitly solved by an observer-like structure. Practical results were presented. Left to ask whether this approach can be generalized to a bigger class of tracking problems?

VIII. Acknowledgements

The authors gratefully acknowledge the collaboration of all partners from University of Karlsruhe (TH), Technical University of Munich (TUM), and University of the German Federal Armed Forces, Munich. This work would not have been possible without the ongoing research of the Transregional Collaborative Research Centre 28 *Cognitive Automobiles*. Both projects cross-fertilized each other and revealed significant synergy.

References

[1] E. Delaleau. Control of flat systems by quasi-static feedback of generalized states. *International Journal of Control*, 71(5):745–765, 1998.

[2] M. Fliess, J. Lévine, P. Martin, and P. Rouchon. Flatness and defect of non-linear systems: introductory theory and examples. *International Journal of Control*, 61(6):1327–1361, 1995.

[3] A. Isidori. *Nonlinear Control Systems*. Springer, 1995.

[4] S. Kammel, J. Ziegler, B. Pitzer, M. Werling, T. Gindele, D. Jagszent, J. Schröder, M. Thuy, M. Goebl, F. v. Hundelshausen, O. Pink, Freese C., and C. Stiller. Team AnnieWAY's autonomous system for the DARPA Urban Challenge 2007. *Journal of Field Robotics*, 2008.

[5] B. Müller and J. Deutscher. Orbital tracking control for car parking via control of the clock. In *ECC, Kos, Greece*, 2007.

[6] Philippe Martin, Pierre Rouchon, and Joachim Rudolph. Invariant tracking. *Control, Optimisation and Calculus of Variations*, 10(1):1–13, jan 2004.

[7] P. Rouchon and J. Rudolph. Invariant tracking and stabilization: Problem formulation and examples. *Lecture notes in control and information sciences*, pages 261–273.